RESEARCH ARTICLE
Cytoskeleton, January 2017 74:40–52 (doi: 10.1002/cm.21334)

X-Rays Effects on Cytoskeleton Mechanics of Healthy and Tumor Cells

Valeria Panzetta,[1†] Marta De Menna,[2†] Ida Musella,[1] Mariagabriella Pugliese,[3] Maria Quarto,[3] Paolo A. Netti,[1,4] and Sabato Fusco[1*]

[1]*Center for Advanced Biomaterials for Health Care@CRIB - Istituto Italiano di Tecnologia, Largo Barsanti e Matteucci n. 53, Napoli 80125, Italy*
[2]*Department of Experimental and Clinic Medicine, University of Catanzaro Magna Graecia, Catanzaro, Italy*
[3]*Dipartimento di Fisica, Università Federico II and INFN-Sezione di Napoli, Monte S. Angelo, Via Cintia, Napoli 80126, Italy*
[4]*Interdisciplinary Research Centre on Biomaterials (CRIB), University of Napoli Federico II, P.le Tecchio 80, Napoli 80125, Italy*

Received 4 April 2016; Revised 9 August 2016; Accepted 15 August 2016
Monitoring Editor: Théry served

Alterations in the cytoskeleton structure are frequently found in several diseases and particularly in cancer cells. It is also through the alterations of the cytoskeleton structure that cancer cells acquire most of their common features such as uncontrolled cell proliferation, cell death evasion, and the gaining of migratory and invasive characteristics. Although radiation therapies currently represent one of the most effective treatments for patients, the effects of X-irradiation on the cytoskeleton architecture are still poorly understood. In this case we investigated the effects, over time of two different doses of X-ray irradiation, on cell cytoskeletons of BALB/c3T3 and Sv40-transformed BALB/c 3T3 cells (SVT2). Biophysical parameters – focal adhesion size, actin bundles organization, and cell mechanical properties – were measured before and after irradiations (1 and 2 Gy) at 24 and 72 h, comparing the cytoskeleton properties of normal and transformed cells. The differences, before and after X-irradiation, were revealed in terms of cell morphology and deformability. Finally, such parameters were correlated to the alterations of cytoskeleton dynamics by evaluating cell adhesion at the level of focal adhesion and cytoskeleton mechanics. X-irradiation modifies the structure and the activity of cell cytoskeleton in a dose-dependent manner. For transformed cells, radiation sensitively increased cell adhesion, as indicated by paxillin-rich focal adhesion, flat morphology, a well-organized actin cytoskeleton, and intracellular mechanics. On the other hand, for normal fibroblasts IR had negligible effects on cytoskeletal and adhesive protein organization. © 2016 Wiley Periodicals, Inc.

Key Words: X-rays; Cytoskeleton; Mechanobiology; Focal Adhesion; Particle Tracking; Microrheology

Introduction

The cytoskeleton (CSK) is a dynamic three-dimensional structure that plays a prominent role in many cell functions and behaviors. Among these, the CSK, through its dynamic rearrangement, is responsible for cell adhesion and shape (Goldman et al., 1996; Mathieu and Loboa, 2012). The functional unit of CSK adhesion to the extracellular matrix (ECM) is represented by the focal adhesions (FAs). These mediate several mechanisms, such as the interactions among cells or between cells and ECM (Ruoslahti and Pierschbacher, 1987), the force transmission and the cytoskeletal organization and signalling (Kanchanawong et al., 2010). Finally, concentration and molecular organization of the CSK components confer to the cells their mechanical properties and their overall deformability. Moreover, it is through the CSK that cells are able to sense the mechanical properties of the surrounding environment. In fact, by altering the cytoskeletal structure and dynamics, mechanical stimuli are recognized by cells and can directly influence cell signalling and gene expression. The global mechanical state of a tissue may influence the properties of its constituents (cells, ECM) and their biophysical parameters (FAs, CSK, stiffness). These, in turn, can trigger a new

Additional Supporting Information may be found in the online version of this article.
[†]These authors have contributed equally to the realization of this work.
*Address correspondence to: Sabato Fusco; Center for Advanced Biomaterials for Health Care@CRIB Istituto Italiano di Tecnologia, Largo Barsanti e Matteucci n. 53, 80125 Napoli, Italy.
E-mail: sabato.fusco@iit.it
Abbreviations used: ECM, Extracellular matrix; FA(s), Focal adhesion(s); IR, Ionizing radiation; MSD(s), Mean squared displacement(s); PTM, Particle tracking microrheology; RBE, Relative Biological Effectiveness; ROS, Reactive oxygen species; SEM, Standard error of the mean.
Published online 17 August 2016 in Wiley Online Library (wileyonlinelibrary.com).

mechanical state transition, which closes the very intricate series of feedback loops between the tissue and its macro and micro constituents. When these loop processes are altered, completely or in part, the tissue architecture degrades and disease may arise. In this context, the maintenance of the CSK architecture is essential for the correct functioning of several cellular processes; therefore, it is well-established that alterations of CSK are commonly associated with a number of diseases, such as: cardiovascular disease syndromes (Honda et al., 1998; Gupta et al., 2010), neurodegenerative diseases (Benítez-King, 2006), cancer (Cross et al., 2008; Fletcher and Mullins, 2010), lung injury (Dudek and Garcia, 2001), and others.

Specifically in the case of cancer, cells acquire several diverse characteristics such as uncontrolled proliferation, cell death evasion, ability to remodel the surrounding matrix, and in the worst-case scenario the capacity to develop metastasis through migration and invasion of distal tissues (Sherr, 1996; Hanahan and Weinberg, 2011). As an essential factor in both proliferation and survival, the CSK is often a target of cancer drugs; in particular, microtubule-targeting drugs are frequently used to control proliferation of numerous cancer cells (Zhou and Giannakakou, 2005). Tumor progression requires cells which are able to develop metastatic focus and in such a process the role of integrins, cadherins and other adhesion proteins is crucial (Hood and Cheresh, 2002). In fact initially in metastasis formation, the cell–cell and cell–matrix adhesions have to be disrupted, allowing release of neoplastic cell from primary tissues (Cross et al., 2008). The alteration in cell adhesion is naturally associated with changes in the concentration and architecture of the CSK (Weber et al., 1974; Beil et al., 2003). Indeed, metastatic cells are generally characterized by reduced stiffness, in terms of CSK mechanics. Moreover, they present an increased migration and invasion ability either because of the active production of proteases (able to digest the surrounding matrix) or to higher self-deformation ability that allows cells to move through the tangle of the matrix (Cross et al., 2008). These observations demonstrate that the alteration of biophysical properties of cells may play a significant role in tumor-genesis and cancer progression.

Nowadays, one of the most effective treatments for cancer is radiation therapy. The ability of ionizing radiation (IR) to induce dramatic consequences for the cell, by promoting the formation of radicals and reactive oxygen species (ROS) which damage DNA and lead to cell death, has been thoroughly investigated (Puck and Marcus, 1956; Puck, 1958; Nüsse, 1981; Iliakis et al., 2003; Suetens et al., 2016). But IR can also target other biologically essential macromolecules, such as lipids and proteins. In particular, many works reported negative effects of IR on plasma membrane. After irradiation plasma membrane loses its barrier function because of variations in the distribution of negative-charge domains (Somosy et al., 1987, 1989) and calcium-content, which modify its permeability (Somosy et al., 1993; Corre et al., 2010). IR affects membrane permeability and fluidity also through two other processes: lipid peroxidase and fragmentation, which induce membrane destabilization and take place in the hydrophobic and hydrophilic moieties, respectively (Shadyro et al., 2002). These alterations are accompanied by morphological changes of membrane and loss of cell–cell contacts (Somosy et al., 1993; Onoda et al., 1999). Somosy et al. (1993) observed in the epithelial layer of the small intestine, a destabilization of tight junctions that increased cell permeability. Trosko stated the importance of alteration in the composition and function of intercellular contacts in cell transformation and carcinogenesis (Trosko, 1996). The close link between plasma membrane lipids and cell CSK elicits an obvious response in CSK organization to IR. In vitro studies indicated that the effects of irradiation depend on cell type and delivered doses. In many types of cells exposure to X-ray produces disruption of the actin CSK, intermediate filaments, and cell contacts (Friedman et al., 1986; Somosy et al., 1995; Onoda et al., 1999). In endothelial cells and endothelial monolayer, radiations determined the formation of persistent actin stress fibers and the redistribution of VE–cadherin junctions by the activation of a rapid RhoA signaling pathway (Gabryś et al., 2007). Other works investigated the effects of radiation on the expression of integrins that, as already stated, are involved in processes such as cell adhesion, migration, and metastasis formation. Several studies showed that irradiation of tumor cells affects integrin expression (Cordes et al., 2003; Abdollahi et al., 2005). The existence of a correlation between changes in the expression of integrins after X-ray irradiation and migratory behavior of tumor cells has been studied. In some cases, higher levels of β3 integrin were accompanied by increased migration after irradiation (Goetze et al., 2007). Eke et al. observed that inhibition of β1 integrin could sensitize head and neck carcinoma cells to radiations (Eke et al., 2012). On the contrary, it seems that for other cells the radiation could diminish the hazard of metastasis and that further cell surface molecules, in addition to β1 integrins, may be relevant for the radiation-dependent regulation of cell migration (Goetze et al., 2007). Many studies also indicated that subcellular compartment changes, induced by radiation exposure, could pass through alterations both at a transcriptional and a translational level. Woloschak et al. demonstrated that IR-induced accumulation of α-tubulin, γ-actin, fibronectin, and repression of β-actin in a dose- and dose rate-dependent way (Woloschak et al., 1990a,b, 1995).

Even though there is a lot of literature which investigates the direct and indirect effects of nonlethal IR on CSK, there are still few reports on how IR affects CSK mechanics, dynamics, and its direct cross-talk with adhesion substrate via FAs. In this paper we investigated the impacts of two different doses of X-irradiation (1 and 2 Gy) on cytoskeletal stiffness of Simian virus 40-transformed BALBc/3T3

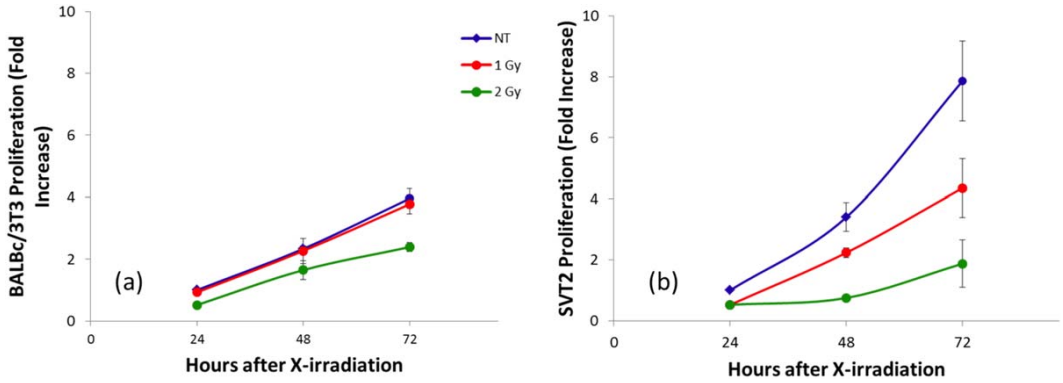

Fig. 1. Effect of X-radiation on BALBc/3T3 and SVT2 cell proliferation. Proliferation of SVT2 cells in culture was inhibited by X-rays in a dose-dependent manner (a). The dose of 1 Gy did not change the proliferation rate of BALBc/3T3, while there was a significant decrease of proliferation when normal fibroblasts were irradiated with 2 Gy of X-rays (b). Values represent the mean of six replicates ± SD. [Color figure can be viewed at wileyonlinelibrary.com]

(SVT2) cells and its normal counterpart BALBc/3T3. The value of 2 Gy was chosen because it is the dose generally employed as a fraction in the radiation treatment plans. Although the energy of the radiation beams used in radiotherapy is of MeV order, the study of the effects of the same dosage at energy of 250 kV is crucial; in fact, at this energy level the X-rays are conventionally used as reference radiation in the calculation of Relative Biological Effectiveness (RBE).

SVT2 cells were chosen because they resemble *in vitro* most of the fundamental characteristics of cancer cells: uncontrolled proliferation, loss of contact inhibition, a less spread morphology, a loss of microfilaments and a less assembled CSK, smaller focal adhesions (FAs) (Akhshi et al., 2014), and an increased motility and deformability. In a previous study (Panzetta et al., 2015), we observed morphological and functional variations after irradiation particularly in SVT2 cells. These changes were shown in terms of reduced proliferative activity, reduced motility and increased cell adhesive area. Here, we investigated whether these effects are also associated to alterations of CSK dynamics, by evaluating cell adhesion at the level of FAs and CSK mechanical properties before and after X-irradiation. Starting from these observations, we considered the cell stiffness evaluation – in connection with the characterization of CSK and FAs – as instructive biophysical markers to distinguish and/or evaluate therapeutic effects between healthy and tumor cells.

Results

The Effect of Radiation on Cell Proliferation

The effectiveness of X-irradiation was checked by evaluating cell viability in both BALBc/3T3 and SVT2 cells. CellTiter 96® AQueous One Solution (Promega) was used to measure cell proliferation in control condition and after irradiation. In control condition, the proliferative capacity of transformed cells was significantly higher than those of BALBc/3T3, as already observed (Carrino and Gershman, 1977). As expected, after X-ray treatment viability of SVT2 cells was significantly reduced in a dose-dependent manner (Fig. 1b), while the proliferation of BALBc3T3 was affected only by the higher dose (Fig. 1a).

Interestingly, the reduced proliferation of SVT2 cells is not because of a lowering of the percentage of cells able to enter S-phase after X-ray treatment (Supporting Information Fig. S1), suggesting that it is more likely that the X-ray treatment is affecting either the S-phase exit or G/2M transition (Nüsse, 1981; Iliakis et al., 2003; Suetens et al., 2016).

The Effect of Radiation on Cell Adhesion

Adhesion experiments were performed to evaluate the adhesive capacity of normal and transformed cells in control and irradiated conditions. Adhesiveness of nonirradiated SVT2 cells was significantly lower than BALBc/3T3, as has already been observed for many malignant cells both in tissues (McCutcheon et al., 1948) and on tissue culture substrates (Franks and Henzell, 1970; Weber et al., 1977). After radiation treatment BALBc/3T3 showed the same adhesion capacity as untreated cells, while irradiated SVT2 cells showed a significant increased adhesion capacity (Fig. 2). In order to better evaluate the dependence of increased adhesion of SVT2 cells on radiation dose, two additional lower doses were tested, 0.25 and 0.5 Gy. A progressive enhancement of adhesion was observed with radiation doses: 0.25 Gy dose did not affect adhesion capacity of transformed cells, while 0.5 Gy did. In fact, the number of cells which adhere after 0.5 Gy was in between the number of cells that adhere after 0.25 and 1 Gy treatment (Supporting Information Fig. S2).

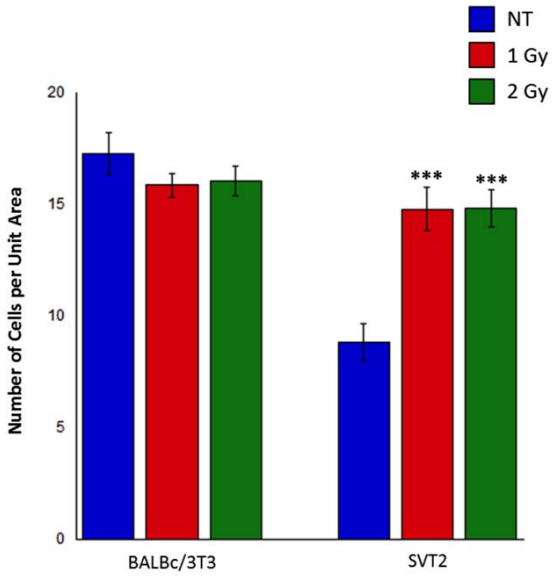

Fig. 2. Effect of X-radiation on BALBc/3T3 and SVT2 cell adhesion to polystyrene dishes. Exposure to 1 and 2 Gy doses of X-ray significantly enhanced SVT2 cell adhesion, but did not affect adhesion of normal fibroblasts. Bars represent the mean of number of adhering cells per unit area ± SEM. Data presented are pooled means of at least 46 images. ***$P < 0.001$ as compared with controls. [Color figure can be viewed at wileyonlinelibrary.com]

The Effect of Radiation on Cell Morphological Changes and FA Size

Using fluorescent microscopy, we further analyzed the morphology and cytoskeletal organization of cells in both control conditions and after treatment with two doses of X-rays. In particular, we analyzed two parameters: (1) The spindle-shape factor, a parameter which gives indirect information about the typical organization of the CSK of fibroblasts into elongated filament bundles (stress fibers) parallel to the polarization direction; (2) The area of single FA, which typically increases in the direction of their associated stress fibers through a process driven by actomyosin-mediated tension. Figures 3 and 4 show morphology and CSK of BALBc/3T3 and SVT2 cells. In control condition, BALBc/3T3 cells were characterized by elongated cell bodies with extended processes which give cells the spindle-like shape, while SVT2 cells showed a round morphology (Fig. 3), probably as a consequence of a reduced adhesion to culture-dishes (Fig. 2). Radiation substantially modifies cell morphology. In fact, 24 h after irradiation SVT2 cells already adopted a more elongated shape which was also maintained at 72 h, as demonstrated by the significant decrease of the spindle factor ($P < 0.001$) both at 1 and 2 Gy doses (Fig. 3i–n), while the shape of BALBc/3T3 was not affected by irradiation (Fig. 3c–h). We observed that transformation is accompanied not only by a reduced adhesiveness, but also by an alteration in the assembly process of FAs; in fact, SVT2 cells show smaller focal adhesion areas compared to normal BALBc3T3. There are some studies which provide evidence that a reduction in cytoskeletal proteins such as actin, tropomyosin and vinculin, is often a key feature of cell transformation (Fernandez et al., 1992). The exposure to X-rays produced – even after 24 h – a significant increase in the focal adhesion area in BALBc/3T3 cells ($P < 0.0001$) and in SVT2 cells ($P < 0.0001$) (Fig. 4). The growth of FAs after X-irradiation was strictly correlated to the cell morphological variations: it was demonstrated that in fibroblasts FAs grown in the direction of major cell-axis, are co-aligned with stress fibers and govern cell polarization, giving the cell its typical elongated shape (Prager-Khoutorsky et al., 2011). Over time FA growth after irradiation was partially recovered in normal cells, even if maintaining a statistical difference with control cells, while persisted in transformed fibroblasts (Fig. 4). The reduced spindle shape factor, the related FAs area growth and the increase of cell spreading area previously reported (Panzetta et al., 2015) implicate major assembly of CSK and a replacement of cortical bundles with a network of stress fibers principally in SVT2 cells.

Cell Mechanics

The mean square displacement (MSD) of nanoprobes embedded in cell provides information about the motion of the particles in cytoplasm and, indirectly, about the mechanics of the cell microenvironment. As a first step, we compared the MSDs of normal and tumor fibroblasts in control condition. Figures 5 and 6 show the cumulative distribution functions of the trajectory in the two cell lines using two different measures: we measured the radius of gyration of particle trajectories (Fig. 5a) and the distance travelled by the MSD at $\tau = 1$ s (Fig. 5b). The two analyses showed similar results: a lognormal distribution of particle displacements in both cells, with higher values in transformed cells. In particular, the radii of gyration in transformed SVT2 cells were significantly higher than in BALBc/3T3, indicating that the particles move further, in accordance with the higher MSD amplitude. These results indicate that the tumorigenicity of cells is probably correlated with a decrease in stiffness and structural density and an increase in intracellular activity.

MSD analysis showed that BALBc/3T3 cells responded rapidly to 2 Gy irradiation, by reducing their intracellular activity at 24 h, while the effect at 1 Gy was less pronounced. The cumulative distribution function of MSD at $\tau = 1$ s shows lower values when BALB/c 3T3 were irradiated with a higher dose at 24 h (Fig. 6a). At 72 h the distribution of particle displacements shifts on the right, but MSDs are restricted to a smaller range of values, so that the mean values of the MSD were the same in control and irradiated conditions ($\approx 8 \times 10^{-4}$ $\mu m^2/s$). The effectiveness of the higher dose of X-rays was also confirmed by the reduction

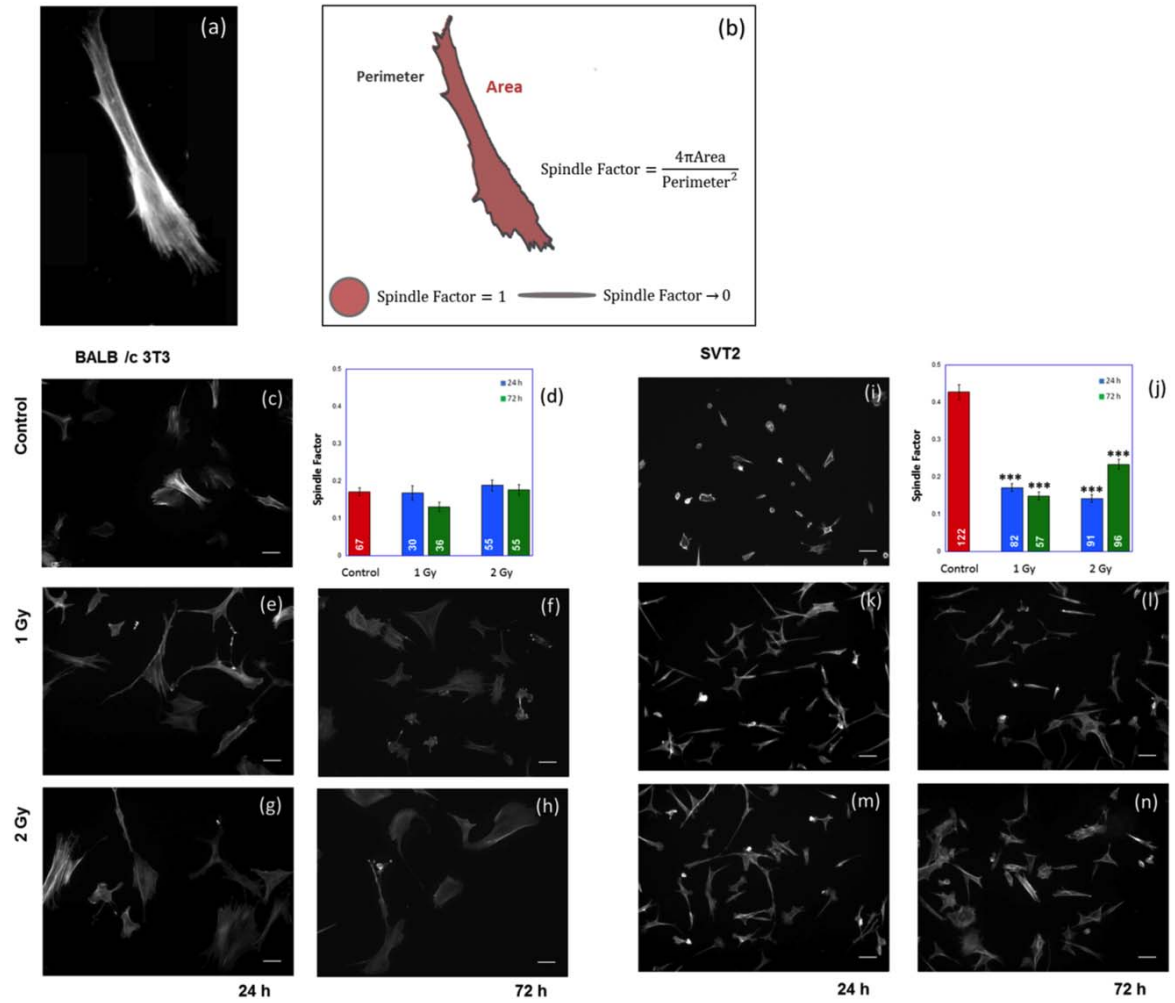

Fig. 3. Representative image of cell morphology (a). Schematic representation of the morphological descriptor, spindle shape factor, which was used in this study (b). The morphology and cytoskeleton in BALBc/3T3 and SVT2 cells are compared before (c–i) and after X-irradiation with doses of 1 Gy (e–f, k–l) and 2 Gy (g–h, m–n). The spindle factor data are presented as mean ± SEM and the number of cells analyzed is indicated in the bars. $^{***}P < 0.001$ as compared with controls. Scale bar, 50 μm. [Color figure can be viewed at wileyonlinelibrary.com]

of the radius of gyration at 24 h (Fig. 6c). Nevertheless, this effect was lost at 72 h (Fig. 6d), indicating a recovery of the initial conditions. However, SVT2 cells already seemed to be responsive to both doses at 24 h and this effect was increased at 72 h. In fact, the MSD curves present reduced amplitudes compared with the curves in control condition (Fig. 7a–b). In addition, the cumulative distribution functions of the MSD and radii of gyration show smaller values at both investigated times and for both X-rays doses (Fig. 7).

Discussion

Tumor progression is associated with the enhanced ability of cells to move and invade adjacent tissues and migrate towards distant sites. Several works demonstrated that the aggressive phenotype of cancer cells is correlated with alterations of adhesion receptors and CSK architecture, deregulation of CSK dynamics mediators and changes in migratory properties (Lark et al., 2005; Desgrosellier and Cheresh, 2010). All these alterations result in variations of cell mechanical characteristics: as cancer cells become more aggressive and invasive, they present decreased cell stiffness. In this context, stiffness is not only a predictor of invasive potential, but it can be used also as a gauge of effectiveness of anti-cancer treatments. In this work we studied the direct effects of X-irradiation on the CSK structure of transformed SVT2 cells and their healthy counterpart, BALBc/3T3 cells, by evaluating, as far as we know for the first time, CSK mechanics and its direct cross-talk with adhesion substrate via FAs. As already stated, the aggressive and malignant phenotype of SVT2 cells is associated with

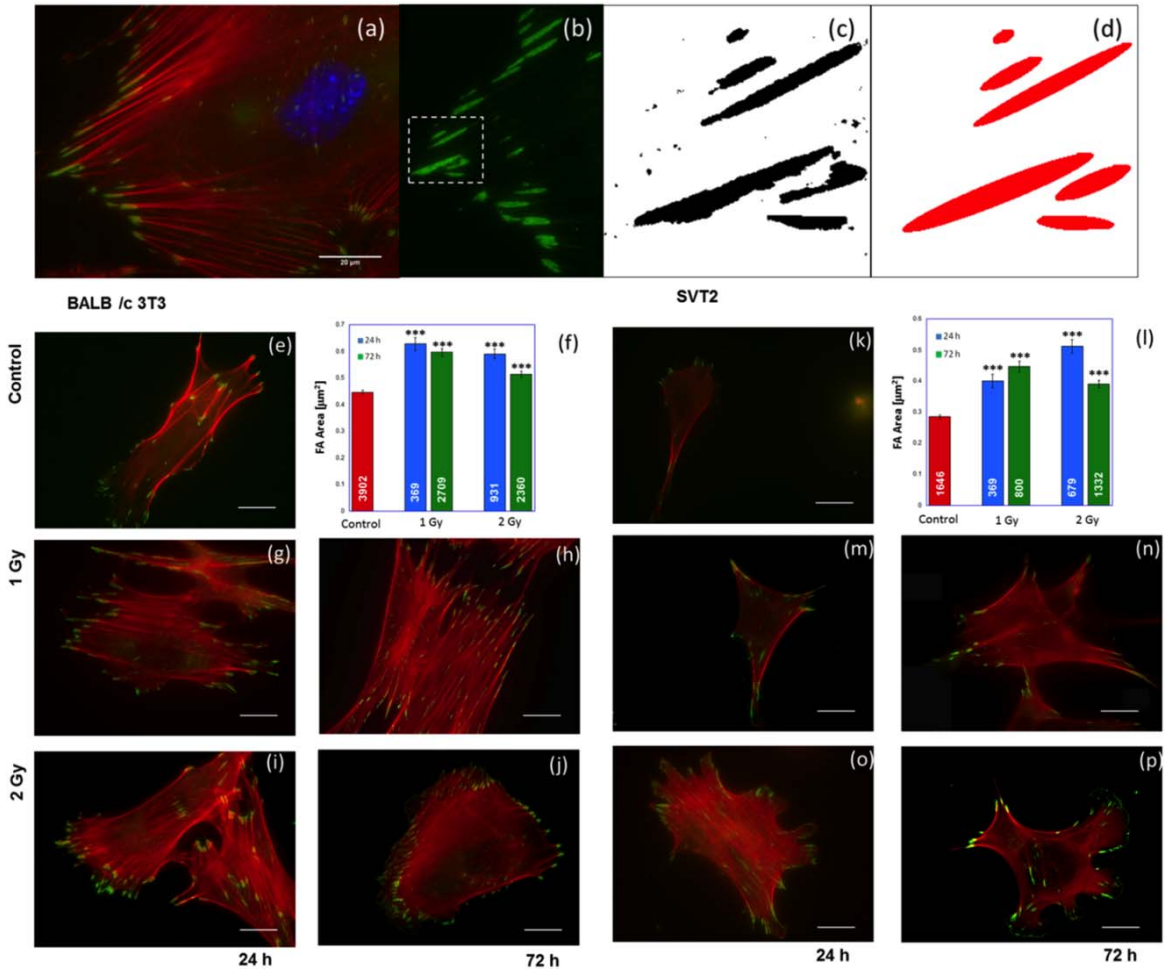

Fig. 4. BALBc/3T3 and SVT2 cells were fixed and stained with phalloidin (red, actin) and immunostained to detect paxillin (green, FAs). Representative images of the organization of actin filaments (a) and FAs (b) of BALBc/3T3 cell, binary image of FAs obtained by thresholding methods (c), best-fit ellipses of FAs (d). Representative images of actin filaments and FAs before (e–k) and after X-irradiation with doses of 1 Gy (g–h, m–n) and 2 Gy (i–j, o–p). Data related to FA areas are presented as mean ± SEM and the number of FAs analyzed is indicated in the bars. $^{***}P < 0.001$ as compared with controls. Scale bar, 10 μm. [Color figure can be viewed at wileyonlinelibrary.com]

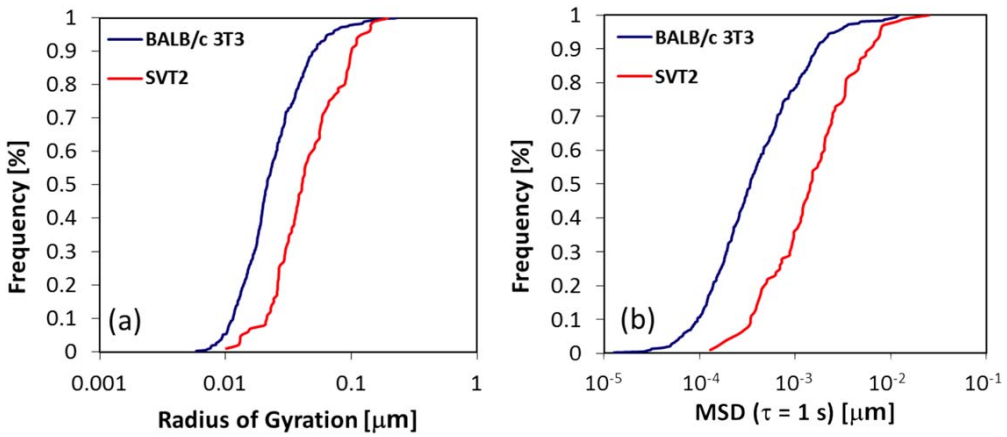

Fig. 5. Cumulative distribution functions of BALB/c3T3 (blue curve) and SVT2 (red curve) cells by calculation of the radius of gyration (a) and MSD (τ=1 s) (b). [Color figure can be viewed at wileyonlinelibrary.com]

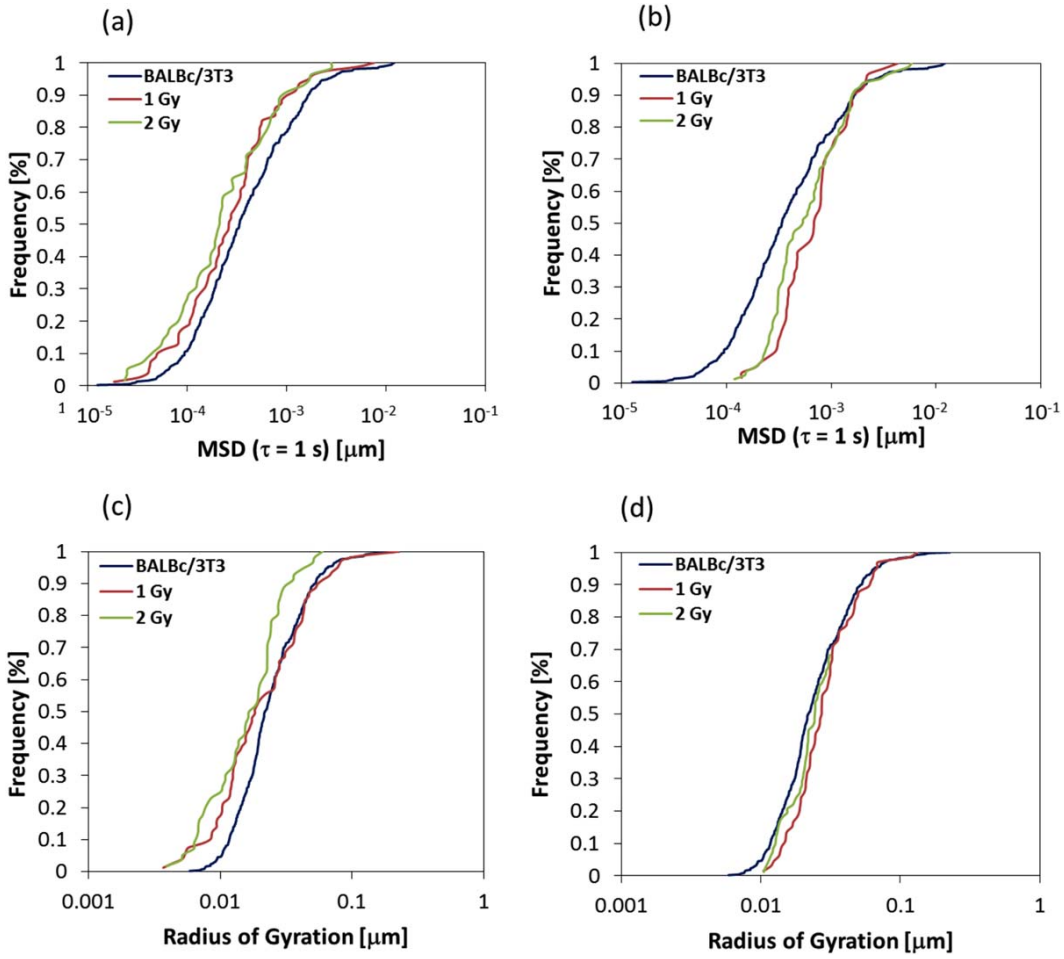

Fig. 6. Cumulative distribution functions of MSD at τ=1 s (a–b) and radius of gyration (c-d) of BALB/c3T3 in control condition (blue curve) and after irradiation with doses of 1 Gy (dark red curve) and 2 Gy (green curve) at 24 h (a,c) and 72 h (b,d). [Color figure can be viewed at wileyonlinelibrary.com]

weak and altered expression of FA proteins. The smaller size of FAs we observed in transformed cells is probably responsible for the modest adhesiveness to the culture dish (Fig. 1), but also for the SVT2 abilities to grow in suspension in a semisolid medium (Stoker et al., 1968) and the loss of adhesion-dependent growth control (Shin et al., 1975). Indeed, the decrease in paxillin level stimulates the disassembly of stable FAs, as demonstrated by the reduced dimensions of FAs in SVT2 cells, shifting the dynamic equilibrium between soluble and assembled FA proteins. The reduction of FA dimensions in SVT2 cells was also associated with an alteration of the CSK protein expression and organization (Fusco et al., 2015). The direct consequence of this dysregulation is a profound reduction in cell–substrate adhesion and a round cellular morphology (Panzetta et al., 2015). As previously reported, we found a strong correlation between cell adhesion to substrate, FAs assembly, actin-CSK architecture and cell mechanical properties (Fusco et al., 2015). We used particle tracking microrheology (PTM) to evaluate the intracellular mechanics of BALB/c3T3 and SVT2 cells, measuring MSDs and radii of gyration of tracked beads. The presence of nonthermal driving forces does not allow us to derive viscoelastic moduli, nevertheless MSD amplitude was shown to be inversely related to intracellular stiffness (Brangwynne et al., 2009). Working on that principle, we performed PTM experiments that showed how MSDs and radii of gyration in SVT2 cells are sensitively higher than in BALB/c3T3 cells, because of a less dense and more active cytoskeletal network. These results suggest that when adhesion and CSK structure are compromised, SVT2 cells result softer and more able to deform, migrate and invade other tissues (Gal and Weihs, 2012), supporting our previous observation of increased motility in transformed cells (Panzetta et al., 2015).

Radiation therapy was established to be an effective treatment for various cancers, but the study of its possible effects on CSK stiffness of cancer cells is limited. Considering the

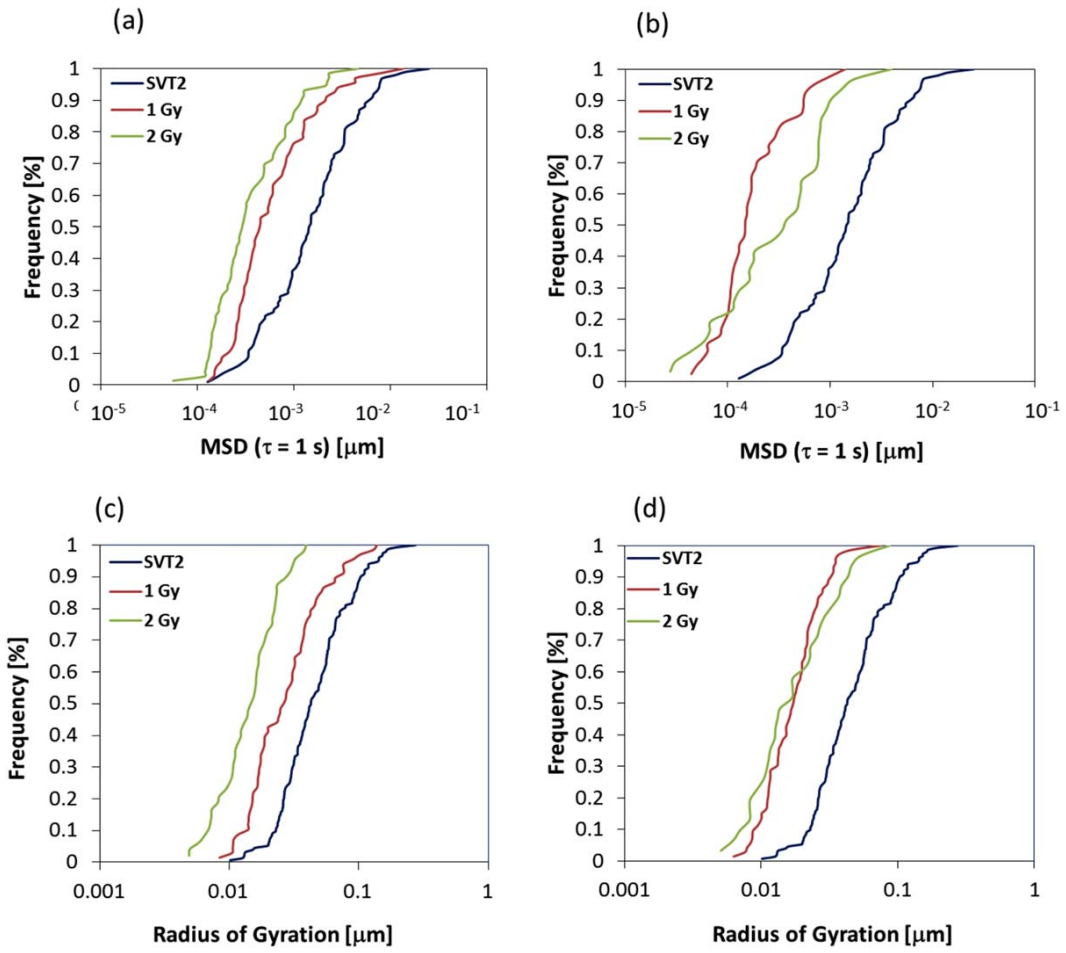

Fig. 7. Cumulative distribution functions of MSD at $\tau = 1$ s (a–b) and radius of gyration (c–d) of SVT2 in control condition (blue curve) and after irradiation with doses of 1 Gy (dark red curve) and 2 Gy (green curve) at 24 h (a,c) and 72 h (b,d). [Color figure can be viewed at wileyonlinelibrary.com]

direct correlation between metastatic, aggressive phenotype of cancer cells and their biophysical and mechanical properties, it is necessary to make an evaluation of the effects of IR on biophysics of cancer cells. The aim of this study was to evaluate for the first time cell response to IR in terms of CSK structuring and stiffness. As previously shown (Panzetta et al., 2015), we observed here that cell proliferation of transformed SVT2 cells is more significantly impaired by X-ray treatment. Possibly the greater radio-sensitivity of transformed cells might be because of a lower expression of adhesion-associated proteins and integrin receptors, as demonstrated by anoikis induction and radio-sensitization in the case of silencing/inhibition of integrins (Eke and Cordes, 2015). Interestingly, our study provided evidence that the 1 Gy dose is sufficient to produce morphological and functional variations of SVT2 cells. In particular, a low-dose of X-irradiation was sufficient to reduce cell viability, increase the spreading area (Panzetta et al., 2015), recover the elongated phenotype and augment FAs size, cell adhesion efficiency and mechanical properties of SVT2 cells. The increase in cell–substrate contact area was an indirect marker of enhanced cell–ECM adhesion, accompanied by receptor recruitment to anchoring sites (integrin-ligand clustering) and then by a local membrane stiffening because of FAs assembly. Consequently, we observed the formation of greater paxillin-containing FAs. The increase of expression level and recruitment of paxillin at FAs sites was naturally associated with the actin- and myosin-containing stress fibers, necessary to give strength for the FAs maturation and maintenance (Zaidel-Bar et al., 2003). Probably the cytoskeletal changes observed after irradiation were related to the central role of the actin in the protection of cells from X-ray-induced oxidative stress. Indeed, Farah et al. demonstrated that actin and its associated proteins are trapped into actin oxidized bodies during oxidative stress events. These bodies protect cells from further oxidative damages and constitute a store of cytoskeletal proteins which guarantee the reassembly of the CSK (Farah et al.,

2011). The enrichment and the organization of stress-fibers and their associated FAs produced, in turn, a stiffening of the CSK, as demonstrated by PTM analysis. In fact, both MSDs and radii of gyration showed reduced values, revealing changes in the internal mechanics and activity of both cell lines, but particularly in transformed cells. The growth of the cell spreading area, the increased actin polymerization and focal adhesions, and the consequent CSK stiffening are probably associated with the reduced motility previously observed (Chen et al., 2008; Fusco et al., 2015; Panzetta et al., 2015). In fact, several studies reported that the overexpression of α-actinin, vinculin, tropomyosin, or other cell adhesion molecules associated with the cytoskeletal network may work as tumor suppressor (Fernandez et al., 1992; Tsukita et al., 1993; Boyd et al., 1995; Yam et al., 2001). It was also demonstrated that the overexpression of individual proteins involved in the stabilization of FAs and CSK, suppressed the ability of cells to migrate or form colonies in soft agar (Cunningham and Gorlin, 1992; Fernandez et al., 1992). However, other studies reported contrasting results about the effects of X-rays on tumorigenic and metastatic behavior of cells. Some works actually showed that a sublethal irradiation augments aggressive and metastatic potential of cancer cells (Wild-Bode et al., 2001; Qian et al., 2002; Camphausen et al., 2001; Cheng et al., 2006). In this regard, a close-relationship between the effects of radiation (on the increased ability of different cell lines to form metastasis) and the integrin overexpression becomes apparent (Onoda et al., 1992; Cordes et al., 2003; Goetze et al., 2007). β1 and β3 integrins were identified as playing a key role not only in adhesion, but also in regulating the expression and the activity of MMP-2 and MMP-9, promoting both migration and proteloytic degradation of ECM (Cordes et al., 2003). Increased integrin expression enhanced the number of cells able to adhere to specific ECM proteins after irradiation (Cordes et al., 2003), in other cases radiation-promoted migration was accompanied by decreased expression of the focal molecules FAK and paxillin (Hwang, 2006). However, other studies demonstrated that X-irradiation effectively suppresses cell migration and invasiveness (Bauman et al., 1999; Goetze et al., 2007; Ogata et al., 2005) and found that carbon beam irradiations are more efficient (Akino et al., 2009; Ogata et al., 2005). When migration was impaired by irradiation, integrin expression and migration were not always correlated thus suggesting that other surface molecules could be involved in the radiation effects on tumor cell migratory behavior. The discrepancy between these results indicates that it is not possible to generalize the results observed, and that radiation-induced effects are necessarily cell line-dependent. In the light of what has been said we can indeed conclude that X-ray restores the biophysical and mechanical properties of SVT2, phenomenon that most likely influences also the proliferation and migration of SVT2 cells after X-ray treatment.

Conclusions

In summary, we found that X-irradiation sensitively increased cell–ECM adhesion, as indicated by paxillin-rich FAs, flat morphology, well-organized actin CSK and, consequently, increased intracellular mechanical properties in transformed cells. Alternatively, IR has negligible effects on cytoskeletal and adhesive protein organization of normal fibroblasts. Therefore, some cell biophysical parameters (such as the stiffness), when accompanied with the characterization of CSK and FAs, may become an instructive marker with which to distinguish and/or evaluate the therapeutic effects between healthy and tumor cells. If correlated to the loss of tumorigenic and metastatic behavior of cancer cells they could, at the same time, be used in a preclinical context to design and optimize radiation therapy treatments.

Materials and Methods

Cell Cultures

Experiments were performed on BALB/c 3T3 and Sv40-transformed BALB/c 3T3 cells (SVT2). Cell lines were cultured at 37°C in 5% CO_2 in Dulbecco's modified Eagle's medium (Euroclone., UK) supplemented with 10% fetal bovine serum (FBS, BioWhatter, MD), 2 mM L-glutamine (Sigma, St. Louis, MO), 1000 U/L penicillin (Sigma, St. Louis, MO), and 100 mg/L streptomycin (Sigma, St. Louis, MO).

Cell X-Rays Irradiation

Cell lines were exposed to X-rays produced by a Thomson tube (TR 300F, 250 kVp, 0.8 Gy/min, Stabilipan, Siemens) and filtered by 1-mm-thick copper foil. Irradiation was performed using the facility installed at the Department of Physics of University of Naples Federico II. Before each irradiation, a physical dosimetry was performed, using an ionization chamber (Victoreen, Mödling, Austria).

Cell Proliferation and Cell Cycle

Cell proliferation was evaluated using CellTiter 96® AQueous One Solution Cell Proliferation Assay (Promega) according to the manufacturer's protocol. 24 h after irradiation, cells were incubated with Cell Titer 96® One Reagent for 90 min, absorbance was then read at 490 nm using a plate reading spectrophotometer. Average absorbance from six replicates for each time and treatment was calculated and expressed as fold change of control at 24 h.

Immunofluorescence Labelling

BALB/c 3T3 and SVT2 cells were cultured at a density of 1000 and 2000 cells/cm^2, respectively. Cells were fixed and immunostained to quantify the spreading area and FA dimensions in control condition and at 24 and 72 h from irradiation. After washing twice with phosphate-buffered

saline (EuroClone), cells were fixed in 4% paraformaldehyde (Sigma-Aldrich) for 20 min, rinsed twice with PBS and permeabilized in 0.1% Triton X 100 (Sigma-Aldrich) for 10 min. Cells were washed three times in PBS and blocked for 15 min in 5% bovine serum albumin (BSA, Sigma-Aldrich). Cells were then incubated for 1 h with anti-paxillin antibody (Abcam), at 1:300 dilution in PBS-BSA. Then, cells were washed for three more times and incubated for 1 h with the secondary antibody, Alexa 488 anti-rabbit (Invitrogen) at 1:500 dilution and Alexa 568 phalloidin (Invitrogen) at 1:40 dilution.

Adhesion Assay

The cell adhesion to polystyrene was studied in control and irradiated conditions. 24 h after irradiation, 2×10^4 not irradiated, irradiated (1 and 2 Gy) cells were washed, trypsinised and plated on 35-mm Petri dishes. After 4 h incubation at 37°C, nonadherent cells were gently washed with PBS and adherent cells were fixed in 4% paraformaldehyde (Sigma-Aldrich) for 20 min and nuclei were counterstained with Hoechst 33342 (Life Technologies). The adherent cells were determined by counting the stained nuclei in a representative unit area (3.6×10^5 μm^2).

Quantification of Cell Morphological Changes and Focal Adhesion Size

Specimens were imaged using an Olympus IX81 inverted microscope and a 10× objective to quantify cell spindle factor and 100× objective to quantify FA area. Fluorescent images were imported into ImageJ software (NIH, Bethesda, MD, USA) for postprocessing analysis and quantification of the cell spindle factor (cellular footprint) and FA area. Individual cells were outlined and changes in cell shape in control and irradiated conditions were quantified by a spindle factor, defined as $4\pi(\text{area})/\text{perimeter}^2$, approaching 1 for a round and 0 for an elongated cell. To quantify the focal adhesion average area, the paxillin images were assembled into a stack. First the stack was Gaussian-filtered using a radius of 30 pixels. This stack was then subtracted from the original stack to reduce diffuse background signal. Adhesions were measured by thresholding the stacks and using an ellipse-fitting function in ImageJ. Objects with area ≤ 0.1 μm^2 were discarded, in order to avoid possible errors because of background noise. Areas of individual focal adhesions were determined for both cell lines in control and irradiated conditions for all investigated time points (24 and 72 h).

Particle Tracking: Ballistic Injection

Carboxyl-modified fluorescent polystyrene particles (0.500 μm diameter, Invitrogen, Molecular Probes) were introduced into the cytoplasm of BALB/c3T3 and SVT2 cells using a ballistic gun (Bio-Rad, Hercules, CA). Helium gas at 450 psi was used to force a macrocarrier disk coated with particles to crash into a stopping screen. The force of the collision was transferred to the particles, causing their dissociation from the macrocarrier and the bombardment of targeted cells. Once bombarded, cells were washed extensively in order to avoid active entering of nanoparticles via endocytosis. The cells were allowed to recover for 24 h, before re-plating. Each dish was supplemented with 2 mL of media and subsequently incubated for 24 h at 37°C, 5% CO_2. After incubation, videos were recorded for a total of 6 s at 50 fps (yielding a total of 300 frames per video) using a fast digital camera (Lambert Instruments, Roden, The Netherlands) attached to a PC and Cam control video capture software. These were taken with an Olympus IX70 (Olympus, Mellville, NY) equipped with a fluorescence mercury lamp (Olympus U-RFL–T) microscope at 100× magnification. Videos were kept short to avoid photobleaching of the particles and active transport of particles caused by cellular motors. To perform experiments under physiological conditions, a microscope stage incubator (Okolab, Naples, Italy) was used to keep cells at 37°C and 5% CO_2, which is supplied as a 5/95% CO_2/air mixture. Ten cells were analyzed for each condition and an average number comprised between 30 and 50 particles was tracked for each cell.

Particle Tracking Microrheology: Mean Square Displacement Method and Radius of Gyration

Particle tracking microrheology (PTM) is a popular technique for probing intracellular dynamics. By using a video particle nano-tracking, the particle displacements are tracked. To generate the point tracking trajectories, the algorithm had to perform two distinct steps: first, it had to detect the points in each frame and then it had to link such points into trajectories. In our self-developed Matlab® (Matlab 7) code, each position was determined by intensity measurements through its centroid, and it was compared frame by frame to produce a trajectory for each particle, based on the principle that the closest positions in successive frames belong to the same particle (proximity principle). After obtaining the trajectories of the nanoparticles, MSDs were calculated from the trajectories of the centroids of the microspheres

$$< \Delta r^2(\tau) > = < [x(t-\tau)-x(t)]^2 + [y(t-\tau)-y(t)]^2 > \quad (1)$$

where means time average, τ is the time scale and t the elapsed time.

The R_g was calculated as the average distance between all measured positions in a trajectory:

$$R_g^2 = \frac{1}{2N^2} \sum_{i=1}^{N} \sum_{j=1}^{N} \left(\vec{R}_i - \vec{R}_j\right)^2 \quad (2)$$

PTM was used to monitor the local viscoelastic properties of living cells, assuming that particles embedded in the cytoplasm are subjected only to thermal fluctuations and that the material is a (hydrodynamic) continuum,

homogeneous and incompressible (Einstein, 1905; Tseng et al., 2002a,b; Squires and Mason, 2009). However, living cells are dynamic and far from equilibrium systems, in cytoplasm not only thermal fluctuations, but also active processes, such as cytoskeletal filaments remodeling and forces generated by motor transport, are present (Hoffman et al., 2006; Brangwynne et al., 2009). This means that the mean squared displacements (MSDs) cannot be related to rheological parameters by using the generalized Stokes-Einstein equation in the case of living cells. However, the MSD gives information about the mechanical properties of cell environment. It was also demonstrated that the MSD amplitude is inversely proportional to the local stiffness in cells (Hoffman et al., 2006; Brangwynne et al., 2009). In order to gather information concerning intracellular structure and mechanics of BALB/c 3T3 and SVT2 cells before and after X-irradiation, we used two parameters: MSD and the radius of gyration (R_g) (Gal et al., 2013). The former is a statistical measure of time-dependent particle displacements; the latter is an averaged measure of the trajectory size.

Statistical Analysis

Data are reported as mean ± standard error of the mean (SEM), unless otherwise indicated. Statistical comparisons were performed with a Student's unpaired test. P values of <0.05 denote statistically significant difference.

Conflict of interest: none.

Acknowledgments

The authors thank Mrs. Alison Sanford and Ms. Roberta Infranca for their precise proofreading.

References

Abdollahi A, Griggs DW, Zieher H, Roth A, Lipson KE, Saffrich R, Gröne H-J, Hallahan DE, Reisfeld RA, Debus J. 2005. Inhibition of αvβ3 integrin survival signaling enhances antiangiogenic and antitumor effects of radiotherapy. Clin Cancer Res 11:6270–6279.

Akhshi TK, Wernike D, Piekny A. 2014. Microtubules and actin crosstalk in cell migration and division. Cytoskeleton 71:1–23.

Akino Y, Teshima T, Kihara A, Kodera-Suzumoto Y, Inaoka M, Higashiyama S, Furusawa Y, Matsuura N. 2009. Carbon-ion beam irradiation effectively suppresses migration and invasion of human non–small-cell lung cancer cells. Int J Radiat Oncol Biol Phys 75:475–481.

Bauman GS, Fisher BJ, McDonald W, Amberger VR, Moore E, Del Maestro RF. 1999. Effects of radiation on a three-dimensional model of malignant glioma invasion. Int J Dev Neurosci 17: 643–651.

Beil M, Micoulet A, von Wichert G, Paschke S, Walther P, Omary MB, Van Veldhoven PP, Gern U, Wolff-Hieber E, Eggermann J. 2003. Sphingosylphosphorylcholine regulates keratin network architecture and visco-elastic properties of human cancer cells. Nat Cell Biol 5:803–811.

Benítez -King G. 2006. Melatonin as a cytoskeletal modulator: implications for cell physiology and disease. J Pineal Res 40:1–9.

Boyd J, Risinger JI, Wiseman RW, Merrick BA, Selkirk JK, Barrett JC. 1995. Regulation of microfilament organization and anchorage-independent growth by tropomyosin 1. Proc Natl Acad Sci 92: 11534–11538.

Brangwynne CP, Koenderink GH, MacKintosh FC, Weitz DA. 2009. Intracellular transport by active diffusion. Trends Cell Biol 19:423–427.

Camphausen K, Moses MA, Beecken W-D, Khan MK, Folkman J, O'Reilly MS. 2001. Radiation therapy to a primary tumor accelerates metastatic growth in mice. Cancer Res 61:2207–2211.

Carrino D, Gershman H. 1977. Division of BALB/c mouse 3T3 and simian virus 40-transformed 3T3 cells in cellular aggregates. Proc Natl Acad Sci 74:3874–3878.

Chen Q, Meng L-h, Zhu C-h, Lin L-p, Lu H, Ding J. 2008. ADAM15 suppresses cell motility by driving integrin α5β1 cell surface expression via Erk inactivation. Int J Biochem Cell Biol 40:2164–2173.

Cheng JC, Chou C, Kuo M, Hsieh C. 2006. Radiation-enhanced hepatocellular carcinoma cell invasion with MMP-9 expression through PI3K/Akt/NF-κB signal transduction pathway. Oncogene 25:7009–7018.

Cordes N, Hansmeier B, Beinke C, Meineke V, Van Beuningen D. 2003. Irradiation differentially affects substratum-dependent survival, adhesion, and invasion of glioblastoma cell lines. Br J Cancer 89:2122–2132.

Corre I, Niaudet C, Paris F. 2010. Plasma membrane signaling induced by ionizing radiation. Mutat Res Rev Mutat Res 704:61–67.

Cross SE, Jin Y-S, Tondre J, Wong R, Rao J, Gimzewski JK. 2008. AFM-based analysis of human metastatic cancer cells. Nanotechnology 19:384003.

Cunningham CC, Gorlin JB. 1992. Actin-binding protein requirement for cortical stability and efficient locomotion. Science 255: 325.

Desgrosellier JS, Cheresh DA. 2010. Integrins in cancer: biological implications and therapeutic opportunities. Nat Rev Cancer 10:9–22.

Dudek SM, Garcia JG. 2001. Cytoskeletal regulation of pulmonary vascular permeability. J Appl Physiol 91:1487–1500.

Einstein A. 1905. UN the movement of small particles suspended in statiunary liquids required by the molecular-kinetic theory of heat.

Eke I, Cordes N. 2015. Focal Adhesion Signaling and Therapy Resistance in Cancer. Elsevier. pp 65–75.

Eke I, Deuse Y, Hehlgans S, Gurtner K, Krause M, Baumann M, Shevchenko A, Sandfort V, Cordes N. 2012. β 1 Integrin/FAK/cortactin signaling is essential for human head and neck cancer resistance to radiotherapy. J Clin Investig 122:1529–1540.

Farah ME, Sirotkin V, Haarer B, Kakhniashvili D, Amberg DC. 2011. Diverse protective roles of the actin cytoskeleton during oxidative stress. Cytoskeleton 68:340–354.

Fernandez JR, Geiger B, Salomon D, Sabanay I, Zöller M, Ben-Ze'ev A. 1992. Suppression of tumorigenicity in transformed cells after transfection with vinculin cDNA. J Cell Biol 119:427–438.

Fletcher DA, Mullins RD. 2010. Cell mechanics and the cytoskeleton. Nature 463:485–492.

Franks L, Henzell S. 1970. The development of "spontaneous" neoplastic transformation in vitro of cells from young and old mice. Eur J Cancer 6:357–364.

Friedman M, Ryan US, Davenport WC, Chaney EL, Strickland DL, Kwock L. 1986. Reversible alterations in cultured pulmonary artery endothelial cell monolayer morphology and albumin permeability induced by ionizing radiation. J Cell Physiol 129:237–249.

Fusco S, Panzetta V, Embrione V, Netti PA. 2015. Crosstalk between focal adhesions and material mechanical properties governs cell mechanics and functions. Acta Biomater 23:63–71.

Gabryś D, Greco O, Patel G, Prise KM, Tozer GM, Kanthou C. 2007. Radiation effects on the cytoskeleton of endothelial cells and endothelial monolayer permeability. Int J Radiat Oncol Biol Phys 69:1553–1562.

Gal N, Lechtman-Goldstein D, Weihs D. 2013. Particle tracking in living cells: a review of the mean square displacement method and beyond. Rheol Acta 52:425–443.

Gal N, Weihs D. 2012. Intracellular mechanics and activity of breast cancer cells correlate with metastatic potential. Cell Biochem Biophys 63:199–209.

Goetze K, Scholz M, Taucher-Scholz G, Mueller-Klieser W. 2007. The impact of conventional and heavy ion irradiation on tumor cell migration in vitro. Int J Radiat Biol 83:889–896.

Goldman RD, Khuon S, Chou YH, Opal P, Steinert PM. 1996. The function of intermediate filaments in cell shape and cytoskeletal integrity. J Cell Biol 134:971–983.

Gupta A, Gupta S, Young D, Das B, McMahon J, Sen S. 2010. Impairment of ultrastructure and cytoskeleton during progression of cardiac hypertrophy to heart failure. Lab Invest 90:520–530.

Hanahan D, Weinberg RA. 2011. Hallmarks of cancer: the next generation. Cell 144:646–674.

Hoffman BD, Massiera G, Van Citters KM, Crocker JC. 2006. The consensus mechanics of cultured mammalian cells. Proc Natl Acad Sci 103:10259–10264.

Honda H, Oda H, Nakamoto T, Honda Z-i, Sakai R, Suzuki T, Saito T, Nakamura K, Nakao K, Ishikawa T. 1998. Cardiovascular anomaly, impaired actin bundling and resistance to Src-induced transformation in mice lacking p130Cas. Nat Genet 19:361–365.

Hood JD, Cheresh DA. 2002. Role of integrins in cell invasion and migration. Nat Rev Cancer 2:91–100.

Hwang SY, Jung JW, Jeong JS, Kim YJ, Oh ES, Kim TH, Kim JY, Cho KH, Han IO. 2006. Dominant-negative Rac increases both inherent and ionizing radiation-induced cell migration in C6 rat glioma cells. International journal of cancer 118:2056–2063.

Iliakis G, Wang Y, Guan J, Wang H. 2003. DNA damage checkpoint control in cells exposed to ionizing radiation. Oncogene 22: 5834–5847.

Kanchanawong P, Shtengel G, Pasapera AM, Ramko EB, Davidson MW, Hess HF, Waterman CM. 2010. Nanoscale architecture of integrin-based cell adhesions. Nature 468:580–584.

Lark AL, Livasy CA, Dressler L, Moore DT, Millikan RC, Geradts J, Iacocca M, Cowan D, Little D, Craven RJ. 2005. High focal adhesion kinase expression in invasive breast carcinomas is associated with an aggressive phenotype. Mod Pathol 18:1289–1294.

Mathieu PS, Loboa EG. 2012. Cytoskeletal and focal adhesion influences on mesenchymal stem cell shape, mechanical properties, and differentiation down osteogenic, adipogenic, and chondrogenic pathways. Tissue Eng B Rev 18:436–444.

McCutcheon M, Coman DR, Moore FB. 1948. Studies on invasiveness of cancer. Adhesiveness of malignant cells in various human adenocarcinomas. Cancer 1:460–467.

Nüsse M. 1981. Cell cycle kinetics of irradiated synchronous and asynchronous tumor cells with DNA distribution analysis and BrdUrd-Hoechst 33258-technique. Cytometry 2:70–79.

Ogata T, Teshima T, Kagawa K, Hishikawa Y, Takahashi Y, Kawaguchi A, Suzumoto Y, Nojima K, Furusawa Y, Matsuura N. 2005. Particle irradiation suppresses metastatic potential of cancer cells. Cancer Res 65:113–120.

Onoda J, Piechocki M, Honn K. 1992. Radiation-induced increase in expression of the α IIbβ3 Integrin in melanoma cells: effects on metastatic potential. Radiat Res 130:281–288.

Onoda JM, Kantak SS, Diglio CA. 1999. Radiation induced endothelial cell retraction in vitro: correlation with acute pulmonary edema. Pathol Oncol Res 5:49–55.

Panzetta V, De Menna M, Bucci D, Giovannini V, Pugliese M, Quarto M, Fusco S, Netti P. 2015. X-ray irradiation affects morphology, proliferation and migration rate of healthy and cancer cells. J Mech Med Biol 15:1540022.

Prager-Khoutorsky M, Lichtenstein A, Krishnan R, Rajendran K, Mayo A, Kam Z, Geiger B, Bershadsky AD. 2011. Fibroblast polarization is a matrix-rigidity-dependent process controlled by focal adhesion mechanosensing. Nat Cell Biol 13:1457–1465.

Puck TT. 1958. Action of radiation on mammalian cells III. Relationship between reproductive death and induction of chromosome anomalies by X-irradiation of euploid human cells in vitro. Proc Natl Acad Sci 44:772–780.

Puck TT, Marcus PI. 1956. Action of X-rays on mammalian cells. J Exp Med 103:653–666.

Qian L-W, Mizumoto K, Urashima T, Nagai E, Maehara N, Sato N, Nakajima M, Tanaka M. 2002. Radiation-induced increase in invasive potential of human pancreatic cancer cells and its blockade by a matrix metalloproteinase inhibitor, CGS27023. Clin Cancer Res 8:1223–1227.

Ruoslahti E, Pierschbacher MD. 1987. New perspectives in cell adhesion: RGD and integrins. Science 238:491–497.

Shadyro O, Yurkova I, Kisel M. 2002. Radiation-induced peroxidation and fragmentation of lipids in a model membrane. Int J Radiat Biol 78:211–217.

Sherr CJ. 1996. Cancer cell cycles. Science 274:1672–1677.

Shin S-I, Freedman VH, Risser R, Pollack R. 1975. Tumorigenicity of virus-transformed cells in nude mice is correlated specifically with anchorage independent growth in vitro. Proc Natl Acad Sci 72:4435–4439.

Somosy Z, Csuka O, Kubasova T, Kovács J, Köteles G. 1989. Surface heterogeneity of tumor cells and changes upon ionizing radiation. Scanning Microsc 3:895–906.

Somosy Z, Kovács J, Siklos L, Köteles G. 1993. Morphological and histochemical changes in intercellular junctional complexes in epithelial cells of mouse small intestine upon X-irradiation: changes of ruthenium red permeability and calcium content. Scanning Microsc 7:961–971.

Somosy Z, Kubasova T, Köteles G. 1987. The effects of low doses of ionizing radiation upon the micromorphology and functional state of cell surface. Scanning Microsc 1:1267–1278.

Somosy Z, Sass M, Bognar G, Kovacs J, Köteles G. 1995. X-irradiation-induced disorganization of cytoskeletal filaments and cell contacts in HT29 cells. Scanning Microsc 9:763–70; discussion 770. 2.

Squires TM, Mason TG. 2009. Fluid mechanics of microrheology. Annu Rev Fluid Mech 42:413.

Stoker M, O'Neill C, Berryman S, Waxman V. 1968. Anchorage and growth regulation in normal and virus-transformed cells. Int J Cancer 3:683–693.

Suetens A, Konings K, Moreels M, Quintens R, Verslegers M, Soors E, Tabury K, Grégoire V, Baatout S. 2016. higher initial Dna Damage and Persistent cell cycle arrest after carbon ion irradiation compared to X-irradiation in Prostate and colon cancer cells. Front Oncol 6:

Trosko JE. 1996. Role of low-level ionizing radiation in multi-step carcinogenic process. Health Phys 70:812–822.

Tseng Y, Kole TP, Lee S-HJ, Wirtz D. 2002a. Local dynamics and viscoelastic properties of cell biological systems. Curr Opin Colloid Interface Sci 7:210–217.

Tseng Y, Kole TP, Wirtz D. 2002b. Micromechanical mapping of live cells by multiple-particle-tracking microrheology. Biophys J 83: 3162–3176.

Tsukita S, Itoh M, Nagafuchi A, Yonemura S. 1993. Submembranous junctional plaque proteins include potential tumor suppressor molecules. J Cell Biol 123:1049–1053.

Weber K, Lazarides E, Goldman R, Vogel A, Pollack R. 1974. Localization and distribution of actin fibers in normal, transformed and revertant cells. Cold Spring Harbor Laboratory Press. pp 363–369.

Weber MJ, Hale AH, Losasso L. 1977. Decreased adherence to the substrate in Rous sarcoma virus-transformed chicken embryo fibroblasts. Cell 10:45–51.

Wild-Bode C, Weller M, Rimner A, Dichgans J, Wick W. 2001. Sublethal irradiation promotes migration and invasiveness of glioma cells Implications for radiotherapy of human glioblastoma. Cancer Res 61:2744–2750.

Woloschak GE, Chang-Liu C-M, Jones PS, Jones CA. 1990a. Modulation of gene expression in Syrian hamster embryo cells following ionizing radiation. Cancer Res 50:339–344.

Woloschak GE, Felcher P, Chang-Liu C-M. 1995. Expression of cytoskeletal and matrix genes following exposure to ionizing radiation: dose-rate effects and protein synthesis requirements. Cancer Lett 92:135–141.

Woloschak GE, Shearin-Jones P, Chang-Liu CM. 1990b. Effects of ionizing radiation on expression of genes encoding cytoskeletal elements: kinetics and dose effects. Mol Carcinog 3:374–378.

Yam JWP, Chan KW, Hsiao W-LW. 2001. Suppression of the tumorigenicity of mutant p53-transformed rat embryo fibroblasts through expression of a newly cloned rat nonmuscle myosin heavy chain-B. Oncogene 20:58–68.

Zaidel-Bar R, Ballestrem C, Kam Z, Geiger B. 2003. Early molecular events in the assembly of matrix adhesions at the leading edge of migrating cells. J Cell Sci 116:4605–4613.

Zhou J, Giannakakou P. 2005. Targeting microtubules for cancer chemotherapy. Curr Med Chem Anticancer Agents 5:65–71.